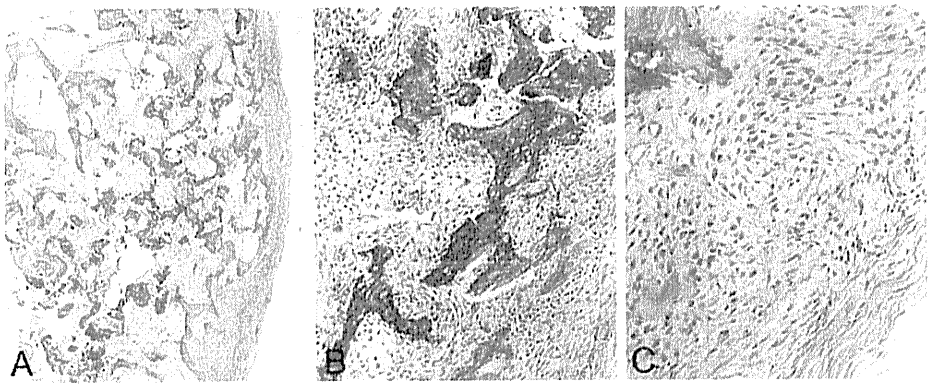

Fig. 4 BPOP shows the three components of cartilage, bone, and spindle cells in differing amounts (**a**). The cartilage and bone interface show irregular ossification and the formed bone trabeculae are characteristically stained blue (**b**). A proliferation of spindle cells without cytologic atypia can be seen (**c**). (H&E; **a** ×50, **b** ×150, **c** ×170)

trabeculae were separated by a fibrous tissue composed of proliferated spindle cells. The spindle cells had no cytologic atypia (Fig. 4c). Osteochondromas are characterized by a cartilage cap and marrow elements between the bone trabeculae, but these features were not observed in this BPOP lesion. Chromosomal abnormality of the lesion was analyzed by the G-banding technique. A fresh sample from the lesion was cultured and metaphase preparations that were stained for Giemsa banding revealed a karyotype with an inversion at the long arm of chromosome 7 [inv (7)(q22q32)]. There is currently no evidence of local recurrence 12 months after the surgery.

Discussion

In the current case, the location and the histological features were typical of BPOP. The typical features of BPOP on radiographs have been reported to be an exophytic bone lesion arising from the cortical surface of the bone, with the finding that BPOP generally does not disrupt the architecture of the underlying bone [3, 4]. In the current case, CT and MRI depicted continuity between the central part of the lesion and the bone marrow of the host bone. Continuity of the central part of the tumor to the underlying bone marrow is usually seen in typical osteochondroma but is not common in BPOP. Such continuity is supposed to be a key radiographic finding of osteochondroma enabling the differentiation between BPOP and osteochondroma [3, 4]. However, corticomedullary continuity has been reported previously [5–8]. The continuity seen in the current case seems to raise an important question regarding the origin of BPOP because BPOP was thought to originate from the surface of the bone or periosteum. An analysis of further cases by CT or MRI is necessary in order to determine whether the continuity is common in BPOP.

In the current case, a chromosomal abnormality of an inversion of the long arm of chromosome 7 [inv (7)(q22q32)] was observed. There have been several reports of rearrangements at the long arm of chromosome 7 (7q22) in cases with myeloproliferative disorder or acute leukemia [12–15]. The chromosomal breakpoint at the long arm of chromosome 7 (7q22) may produce abnormalities involving a tumor suppressor gene [12]. Inversion at the long arm of chromosome 7 (7q22) has also been reported in cases with acute lymphoblastic leukemia and myelodysplasia [13, 14]. Therefore, in the current case, an inversion of chromosome 7 could contribute to the pathogenesis due to the neoplastic nature of BPOP. Previously, a translocation between chromosomes 1 and 17 [t(1;17)(q32;q21)], or its variant translocations, has been reported to be a unique abnormality in BPOP [9]. Another report has described the translocation between chromosomes 1 and 17 [t(1;17)(q42;q23)] [10]. On the other hand, some researchers have described an abnormality of additional ring chromosomes derived from chromosome 12 [11]. Taken together, the translocation between chromosomes 1 and 17 reported in other BPOP cases may not be the only cause, even though chromosome translocation is typical. Furthermore, we speculate that a variant chromosomal abnormality in BPOP may be related to the different phenotypes observed such as the presence of corticomedullary continuity.

Surgical excision is the recommended treatment for BPOP [3]. Recurrence has been reported in at least half of all cases [2]. Because of the high rate of recurrence, cryotherapy has also been recommended as an adjuvant treatment [16]. On the other hand, another study reported a low rate of recurrence comprising only 1 out of 10 patients with BPOP [3]. The authors of that report suggested that wide resection including the pseudocapsule periosteal tissue beneath the lesion and the adjacent cortex of the host bone is important. Moreover, the method of resection reduces the risk of recurrence [3]. In line with these conclusions, wide resection including the overlying fibrous tissue and the cortex of the host bone nearby was performed in the current BPOP case. There has been no recurrence for 1 year

since the resection. However, further follow up is necessary because the period between the initial surgery and recurrence has been reported to range from 2 months to 2 years [9].

In summary, we report a case of BPOP with typical histological features. The continuity of the central part of the lesion to the bone marrow of the host bone was observed. In general, the presence of a corticomedullary continuity in BPOP is uncommon, but has been reported previously [5–8]. Therefore, confirmation is required as to whether the corticomedullary continuity is in fact a common feature in BPOP. In addition, the chromosomal abnormality in the current case involving an inversion of chromosome 7 rather than the previously reported translocation between chromosomes 1 and 17 may suggest that translocation may not be the only cause of BPOP.

Acknowledgments We thank Miss K. Miller (Royal English Language Centre, Fukuoka, Japan) for revising the English used in this manuscript.

References

1. Nora FE, Dahlin DC, Beabout JW. Bizarre parosteal osteochondromatous proliferations of the hands and feet. Am J Surg Pathol. 1983;7(3):245–50.
2. Meneses MF, Unni KK, Swee RG. Bizarre parosteal osteochondromatous proliferation of bone (Nora's lesion). Am J Surg Pathol. 1993;17(7):691–7.
3. Michelsen H, Abramovici L, Steiner G, Posner MA. Bizarre parosteal osteochondromatous proliferation (Nora's lesion) in the hand. J Hand Surg Am. 2004;29(3):520–5.
4. Tannenbaum DA, Biermann JS. Bizarre parosteal osteochondromatous proliferation of bone. Orthopedics. 1997;20(12):1186–8.
5. Rybak LD, Abramovici L, Kenan S, Posner MA, Bonar F, Steiner GC. Cortico-medullary continuity in bizarre parosteal osteochondromatous proliferation mimicking osteochondroma on imaging. Skeletal Radiol. 2007;36(9):829–34.
6. Bell WC, Klein MJ, Pitt MJ, Siegal GP. Molecular pathology of chondroid neoplasms: part 1, benign lesions. Skeletal Radiol. 2006;35(11):805–13.
7. Sundaram M, Wang L, Rotman M, Howard R, Saboeiro AP. Florid reactive periostitis and bizarre parosteal osteochondromatous proliferation: pre-biopsy imaging evolution, treatment and outcome. Skeletal Radiol. 2001;30(4):192–8.
8. Dhondt E, Oudenhoven L, Khan S, Kroon HM, Hogendoorn PC, Nieborg A, et al. Nora's lesion, a distinct radiological entity? Skeletal Radiol. 2006;35(7):497–502.
9. Nilsson M, Domanski HA, Mertens F, Mandahl N. Molecular cytogenetic characterization of recurrent translocation breakpoints in bizarre parosteal osteochondromatous proliferation (Nora's lesion). Hum Pathol. 2004;35(9):1063–9.
10. Endo M, Hasegawa T, Tashiro T, Yamaguchi U, Morimoto Y, Nakatani F, et al. Bizarre parosteal osteochondromatous proliferation with a t(1;17) translocation. Virchows Arch. 2005;447(1):99–102.
11. Zambrano E, Nosé V, Perez-Atayde AR, Gebhardt M, Hresko MT, Kleinman P, et al. Distinct chromosomal rearrangements in subungual (Dupuytren) exostosis and bizarre parosteal osteochondromatous proliferation (Nora lesion). Am J Surg Pathol. 2004;28(8):1033–9.
12. Forrest DL, Lee CL. Constitutional rearrangements of 7q22 in hematologic malignancies. a new case report. Cancer Genet Cytogenet. 2002;139(1):75–7.
13. Orye E, Van Bever H. Paracentric inversions: two new familial cases, inv (7)(q22q11) and inv (11)(q23q13). J Med Genet. 1983;20(3):231.
14. Johnson EJ, Scherer SW, Osborne L, Tsui LC, Oscier D, Mould S, et al. Molecular definition of a narrow interval at 7q22.1 associated with myelodysplasia. Blood. 1996;87(9):3579–86.
15. Stanley WS, Burkett SS, Segel B, Quiery A, George B, Lobel J, et al. Constitutional inversion of chromosome 7 and hematologic cancers. Cancer Genet Cytogenet. 1997;96(1):46–9.
16. Lindeque BG, Simson IW, Fourie PA. Bizarre parosteal osteochondromatous proliferation of a phalanx. Arch Orthop Trauma Surg. 1990;110(1):58–60.

Original Article

The Akt/Mammalian Target of Rapamycin Pathway Is Activated and Associated With Adverse Prognosis in Soft Tissue Leiomyosarcomas

Nokitaka Setsu, MD[1]; Hidetaka Yamamoto, MD, PhD[1]; Kenichi Kohashi, MD, PhD[1]; Makoto Endo, MD[1]; Shuichi Matsuda, MD, PhD[2]; Ryohei Yokoyama, MD, PhD[3]; Kenichi Nishiyama, MD, PhD[4]; Yukihide Iwamoto, MD, PhD[2]; Yoh Dobashi, MD, PhD[5]; and Yoshinao Oda, MD, PhD[1]

BACKGROUND: The Akt/mammalian target of rapamycin (mTOR) pathway mediates cell survival and proliferation and contributes to tumor progression. Soft tissue leiomyosarcoma continues to show poor prognosis, and little is known about its mechanisms of tumor progression. Here the authors investigated the significance of activation of the Akt/mTOR pathway in soft tissue leiomyosarcomas. **METHODS:** The phosphorylation status of Akt, mTOR, S6, and the eukaryotic translation initiation factor 4E-binding protein (4E-BP1) and the protein expression of phosphatase and tensin homologue (PTEN) were assessed by immunohistochemistry in 145 formalin-fixed paraffin-embedded samples of soft tissue leiomyosarcoma including 129 primary tumors. The expression of phosphorylated Akt and mTOR in comparison with their total forms was assessed by Western blot analysis in 13 frozen samples, which were paired with normal tissue samples. Moreover, 39 frozen tumor samples were analyzed for *PIK3CA* and *AKT1* gene mutation. **RESULTS:** Immunohistochemically, phosphorylated forms of Akt, mTOR, S6, and 4E-BP1 were positive in 78.3%, 72.6%, 74.5%, and 70.5% of the samples, respectively. These results were correlated with each other, and associated with higher mitotic activity and adverse prognosis. Decreased expression of PTEN was recognized in only 19.7% and had no statistically significant correlation with Akt or other molecules. Immunoblotting showed a high degree of Akt and mTOR phosphorylation in tumor samples compared with that in non-neoplastic tissue. Mutational analysis failed to reveal any *PIK3CA* or *AKT1* mutations around the hot spots. **CONCLUSIONS:** The Akt/mTOR pathway was activated in most cases of soft tissue leiomyosarcoma and associated with worse clinical behavior and aggressive pathological findings. ***Cancer* 2011;000:000–000.** *© 2011 American Cancer Society.*

KEYWORDS: soft tissue neoplasms, leiomyosarcoma, Akt, mTOR, mutation.

INTRODUCTION

Leiomyosarcoma (LMS) of soft tissue origin accounts for as many as 16% of all soft tissue sarcomas (STSs).[1] Nevertheless, little is known about the mechanisms of tumor progression of LMS, and its prognosis is still adverse.

Phosphoinositide 3-kinase (PI3K) and the downstream Akt/mammalian target of rapamycin (mTOR) pathway have an essential role in modulating cellular functions in response to extracellular signals such as growth factors and cytokines.[2,3] PI3K activates the downstream serine-threonine kinase Akt. Akt in turn phosphorylates many downstream molecules involved in the regulation of cellular functions. One of the substrates of Akt, mTOR, is a key effector of protein synthesis, and its downstream targets include ribosomal protein S6 kinase and the eukaryotic translation initiation factor 4E-binding protein (4E-BP1).[4,5] Phosphorylation of 4E-BP1 upregulates protein translation by releasing eukaryotic

Corresponding author: Yoshinao Oda, MD, PhD, Department of Anatomic Pathology, Graduate School of Medical Sciences, Kyushu University, Maidashi 3-1-1, Higashi-ku, Fukuoka 812-8582, Japan; Fax: (011) 81-92-642-5968; oda@surgpath.med.kyushu-u.ac.jp

[1]Department of Anatomic Pathology, Graduate School of Medical Science, Kyushu University, Fukuoka, Japan; [2]Department of Orthopedic Surgery, Graduate School of Medical Science, Kyushu University, Fukuoka, Japan; [3]Department of Orthopedics, National Kyushu Cancer Center, Fukuoka, Japan; [4]Department of Pathology, National Kyushu Cancer Center, Fukuoka, Japan; [5]Department of Pathology, Saitama Medical Center, Jichi Medical University, Saitama, Japan

We thank the Research Support Center, Graduate School of Medical Sciences, Kyushu University for technical support.

DOI: 10.1002/cncr.26448, **Received:** March 14, 2011; **Revised:** May 30, 2011; **Accepted:** June 21, 2011, **Published online** in Wiley Online Library (wileyonlinelibrary.com)

translation initiation factor 4E. Activation of S6 kinase and phosphorylation of its substrate S6 contribute to the regulation of cell size and cell proliferation.[6]

The Akt/mTOR pathway has been shown to be highly activated in various malignant tumors. Some authors investigated the involvement of the Akt/mTOR pathway in series of STSs, with compatible results indicating that activation of Akt was correlated with worse prognosis[7] and activation of Akt was correlated with a higher probability of metastasis.[8] To date, however, there has been no investigation focused on an LMS series.

Phosphatase and tensin homologue (PTEN), known as a tumor suppressor, can antagonize signaling through PI3K, and thus is a potential inhibitor of the Akt/mTOR pathway.[9] Mutations or loss of heterozygosity of the *PTEN* gene and resulting decrease of PTEN protein expression could activate this pathway. In our preliminary study, *PTEN* mutation was identified in 2 of 13 LMS cases that had showed normal protein expression, and no homozygous deletion or promoter methylation was detected.[10] This result indicates that PTEN protein expression status rather than *PTEN* gene alteration should be analyzed in LMS.

Recent studies have revealed another activator of the Akt/mTOR pathway: mutations in *PIK3CA* and *AKT1*. The *PIK3CA* gene codes for p110alpha, the catalytic subunit of class Ia PI3K. *PIK3CA* mutations in human neoplasms have gained increasing attention since the landmark study of Samuels et al,[11] in which "hot spots" of mutations were reported in exon 9 (E542K, E545K) and exon 20 (H1047R), and these mutations were confirmed to increase the lipid kinase activity of PI3K in vitro.[12,13] *AKT1* mutations have been reported to be situated in the pleckstrin homology domain (E17K) and increase Akt kinase activity.[14] These mutations have not been analyzed in LMS or any other STS.

In the present study, we investigated the phosphorylation status of Akt, mTOR, S6, and 4E-BP1 in a large series of soft tissue LMSs, and evaluated the relationship between Akt/mTOR pathway activation and the clinical and histopathological features. In addition, we analyzed PTEN protein expression by immunohistochemistry and the existence of mutations of the *AKT1* and *PIK3CA* genes by direct sequencing to identify the mechanisms of activation of the Akt/mTOR pathway.

MATERIALS AND METHODS

Patients and Materials

We used the samples of soft tissue LMS registered in the files of the Department of Anatomic Pathology, Graduate School of Medical Sciences, Kyushu University, Fukuoka, Japan. Each tumor was classified according to its location and histology by reference to the World Health Organization classification.[15] Tumor location was categorized into somatic soft tissue (proximal or distal), retroperitoneum, and large vessels. LMS confined to the dermis (true cutaneous LMS) and LMS in the abdominal cavity or external genitals were excluded from this series. All the cases were reviewed based on histological examinations with hematoxylin & eosin (H&E) staining and on an immunohistochemically positive reaction of at least 2 of the following markers: alpha-smooth muscle actin, desmin, and muscle-specific actin. In addition, we carefully excluded gastrointestinal stromal tumors by histological examination and immunostaining with c-kit (CD117) and CD34. If the tumor specimen showed a pleomorphic area of 50% or more, the tumor was defined as a pleomorphic leiomyosarcoma.[16] Specimens with a pleomorphic area of <50% were also categorized as "pleomorphic area <50%." If the tumor showed a >50% area with prominent myxoid stroma, it was described as having a "myxoid area." Inflammatory LMS and LMS with osteoclast-type giant cells were also categorized. Three tumors that had been resected after chemotherapy and showed minimal degeneration because of chemotherapy were included in our series, and they were evaluated considering their corresponding biopsy materials. Histological grade was evaluated according to the grading system of the French Federation of Cancer Centers.[17] Moreover, the staging system described in the sixth edition of the American Joint Committee on Cancer (AJCC) manual[18] as well as that described in the seventh edition[17] were also used. MIB-1 expression was evaluated by immunohistochemistry, and the percentage of MIB-1–immunopositive cells was referred to as the MIB-1 labeling index (LI).

One-hundred forty-five formalin-fixed paraffin-embedded samples of soft tissue LMS from 129 patients (129 primary tumors, 6 metastatic lesions in lung, bone, and subcutaneous tissue, and 10 local recurrences) were prepared for immunohistochemical study. These samples had been obtained from biopsy specimens or surgically resected tumors. Samples after chemotherapy were not included in immunohistochemistry. Survival data were available for 116 LMS cases (90%), with a follow-up ranging from 1 to 346 (median 27) months. Western blotting was performed on 13 frozen samples of LMS, which were paired with normal tissue samples (skeletal muscle). DNA extracted from frozen tumor samples from 39 cases were analyzed for gene mutations.

Eight benign soft tissue smooth muscle tumors (6 leiomyomas and 2 angioleiomyomas) were also examined

immunohistochemically for comparison. None of the benign tumors revealed atypia, mitotic figures, or tumor necrosis. One case of leiomyoma had arisen in the retroperitoneum, and the others had been found in subcutaneous tissue. The institutional review board at Kyushu University approved this study (permission code: 22-73).

Immunohistochemistry

Formalin-fixed, paraffin-embedded tissue was cut at 3 μm. Antigen retrieval was carried out by boiling the slides with 10 mM sodium citrate (pH 6.0) or Target Retrieval Solution (DAKO, Carpinteria, Calif). The following rabbit monoclonal antibodies were used as the primary antibody: PTEN (1:50), phosphorylated (p) Akt (Ser473) (1:50), pmTOR (Ser2448) (1:50), pS6 (Ser235/236) (1:50), and p4E-BP1 (Thr37/46), (1:400) (Cell Signaling Technology, Danvers, Mass). The immune complex was observed with the DAKO EnVision Detection System. Negative controls were obtained by incubating the slides with nonrelevant antibodies of the same isotype. Coexistent endothelial cells (ECs) were evaluated as a positive internal control, because Akt/mTOR pathway was reported to be activated in ECs.[19]

The percentage of immunoreactive cells and staining intensity compared with those of the ECs adjacent to the tumor cells were evaluated in the most representative areas, with reference to the evaluation method of Dobashi et al.[8] The proportion of significantly immunoreactive cells was scored 0 to 2: 0, <10%; 1, 10% to 50%; 2, >50%. *Significant* was defined as definite staining with higher intensity than that observed in ECs adjacent to the tumor cells. When the score was ≥1, the samples were judged as positive, and thus Akt, mTOR, S6, or 4E-BP1 was defined as activated. PTEN expression was judged as decreased when the tumor cells did not show any staining.

Western Blotting

Protein was extracted from frozen samples using lysis buffer (PRO-PREP Protein Extraction Solution; iNtRON Biotechnology, Seongnam, South Korea), separated by sodium dodecyl sulfate-polyacrylamide gel electrophoresis, and transferred to polyvinylidene difluoride membranes. One tumor sample was applied to each membrane as a loading control for quantitative analysis. Membranes were blocked with 5% nonfat dry milk. Rabbit monoclonal antibodies for pAkt (Ser473), pmTOR (Ser2448), pS6 (Ser235/236), pan-Akt, and pan-mTOR (1:1000) (Cell Signaling Technology) were used as primary antibodies. As internal controls, antiactin (1:10,000) (MP Biomedicals, Irvine, Calif) and antiglyceraldehyde 3-phosphate dehydrogenase (1:5000) (Santa Cruz Biotechnology, Santa Cruz, Calif) mouse monoclonal antibodies were used. Membranes were next incubated with antirabbit immunoglobulin (IgG) (Cell Signaling Technology) or antimouse IgG1 (Santa Cruz Biotechnology). All membranes were observed using ECL Plus (GE Healthcare, Buckinghamshire, UK). Images were analyzed using LAS-4000 Image Reader and MultiGauge version 3.0 (Fujifilm, Tokyo, Japan).

Table 1. Primer Sequences Used in Polymerase Chain Reaction for Mutation Screening

Gene, Exon	Sequence	Size, bp
PIK3CA, exon 9	F: GCTAGAGACAATGAA TTAAGGGAAA; R: AGC ACTTACCTGTGACTCCA	122
PIK3CA, exon 20	F: AACTGAGCAAGAG GCTTTGG; R: CTTTTCAG TTCAATGCATGCTG	122
AKT1, exon 2	F: AGTGTGCGTGGCTCTC ACCA; R: AGCCTCACGTT GGTCCACAT	140

Abbreviations: F, forward; R, reverse.

Mutational Analysis

DNA was extracted using the Qiagen DNA Mini Kit (QIAGEN, Valencia, Calif). The primer sequences are summarized in Table 1. They were synthesized by Genenet Co. (Fukuoka, Japan), with partial reference to the primers of Dunlap et al.[20] *PIK3CA* exons 9 and 20 and *AKT1* exon 2 were amplified by polymerase chain reaction (PCR) in 39 cases at an annealing temperature of 57°C. Bidirectional sequencing was performed on an ABI 3130 sequencer using the Big-Dye terminator method (with the same primers as for PCR, Table 1).

Statistical Analysis

Continuous variables are presented as mean ± standard deviation. Chi-square test, Fisher exact test, and Mann-Whitney *U* test were used as appropriate to evaluate the association between 2 variables. Tukey multiple comparison test was applied when needed. The survival correlations were illustrated with Kaplan-Meier curves, and survival analyses were performed by using the log-rank test. In the multivariate analysis, the Akaike Information Criterion was calculated, and the Weibull model was chosen as the appropriate parametric model. A 2-sided *P* value of <.05 was considered to indicate statistical significance.

Table 2. Clinicopathological Parameters and Survival Analysis in 129 Primary Tumors

Parameter	Group	No.	%	Analyzed Groups	Disease-Specific Survival, *P*	Event-Free Survival, *P*
Sex	Male	65	50.4		.8615	.3573
	Female	64	49.6			
Age [mean, 60 years; range, 21-95 years]	<60 years	64	49.6		.3421	.5426
	≥60 years	65	50.4			
Depth	Superficial	39	30.2	In all the cases	.0173[a]	.0144[a]
	Deep	73	56.6	In somatic cases, P and D	.0185[a]	.0660
	N/A	17	13.2			
Diameter	<5 cm	44	34.1		.0467[a]	.0370[a]
	≥5 cm	74	57.4			
	N/A	11	8.5			
Location	D	21	16.3			
	P	72	55.8	P vs D	.1206	.2861
	R	32	24.8	R vs P and D	.5286	.0936
	V	4	3.1	V vs P and D	.2014	.0446[a]
Surgical margin	Negative	83	64.3	In all the cases	.2049	.0268[a]
	Positive	36	27.9	In somatic cases, P and D	.2792	.0387[a]
	N/A	10	7.8	In other cases, R and V	.9234	.9905
Subtype	C	70	54.2			
	Pleo.	35	27.1	Pleo. vs C	.0005[a]	.0546
	LMS with <50% pleomorphic area	11	8.5	Pleo. <50% vs C	.0758	.2510
	LMS with giant cell	6	4.7	Giant cell vs C	.0178[a]	.0001[a]
	LMS with myxoid area	5	3.9	Myxoid area vs C	.0276[a]	.4034
	Inflammatory leiomyosarcoma	2	1.6	Inflammatory vs C	N/A[b]	.7202
Necrosis	None	68	52.7		<.0001[a]	.0064[a]
	<50%	55	42.6			
	≥50%	6	4.7			
Mitotic activity	0-9/10 HPF	62	48.1		.0002[a]	.0063[a]
	10-19/10 HPF	28	21.7			
	≥20/10 HPF	39	30.2			
MIB-1 LI	<30%	52	40.3		.0113[a]	.0238[a]
	≥30%	67	51.9			
	N/A	10	7.8			
FNCLCC	1	41	31.8		<.0001[a]	.0005[a]
	2	52	40.3			
	3	36	27.9			
AJCC 6th ed	I	41	31.8		.0016[a]	.0018[a]
	II	55	42.6			
	III	17	13.2			
	IV	7	5.4			
	N/A	9	7.0			
AJCC 7th ed	I	13	10.1		.0907	.0991
	II	81	62.8			
	III	19	14.7			
	IV	7	5.4			
	N/A	9	7.0			

Abbreviations: AJCC, American Joint Committee on Cancer; C, classical leiomyosarcoma; D, distal extremities; FNCLCC, French Federation of Cancer Centers; HPF, high-power fields; LI, labeling index; LMS, leiomyosarcoma; N/A, not available; P, proximal extremities and trunk; Pleo., pleomorphic leiomyosarcoma; Pleo. <50%, leiomyosarcoma with <50% pleomorphic area; R, retroperitoneum; V, large vessels.

[a] Statistically significant.

[b] *P* value could not be calculated because all the inflammatory LMS cases were alive at the final follow-up.

RESULTS

Patients and Clinicopathological Parameters

The clinicopathological data and the results of the survival analysis for the 129 primary tumors are summarized in Table 2, and representative H&E staining of each histological type is shown in Figure 1. The information of adjuvant therapy was not included because of its diversity and biased indication. About 1/4 of the tumors were retroperitoneal, and slightly more of these cases were in women than in men (male, 14; female, 18). With respect to the

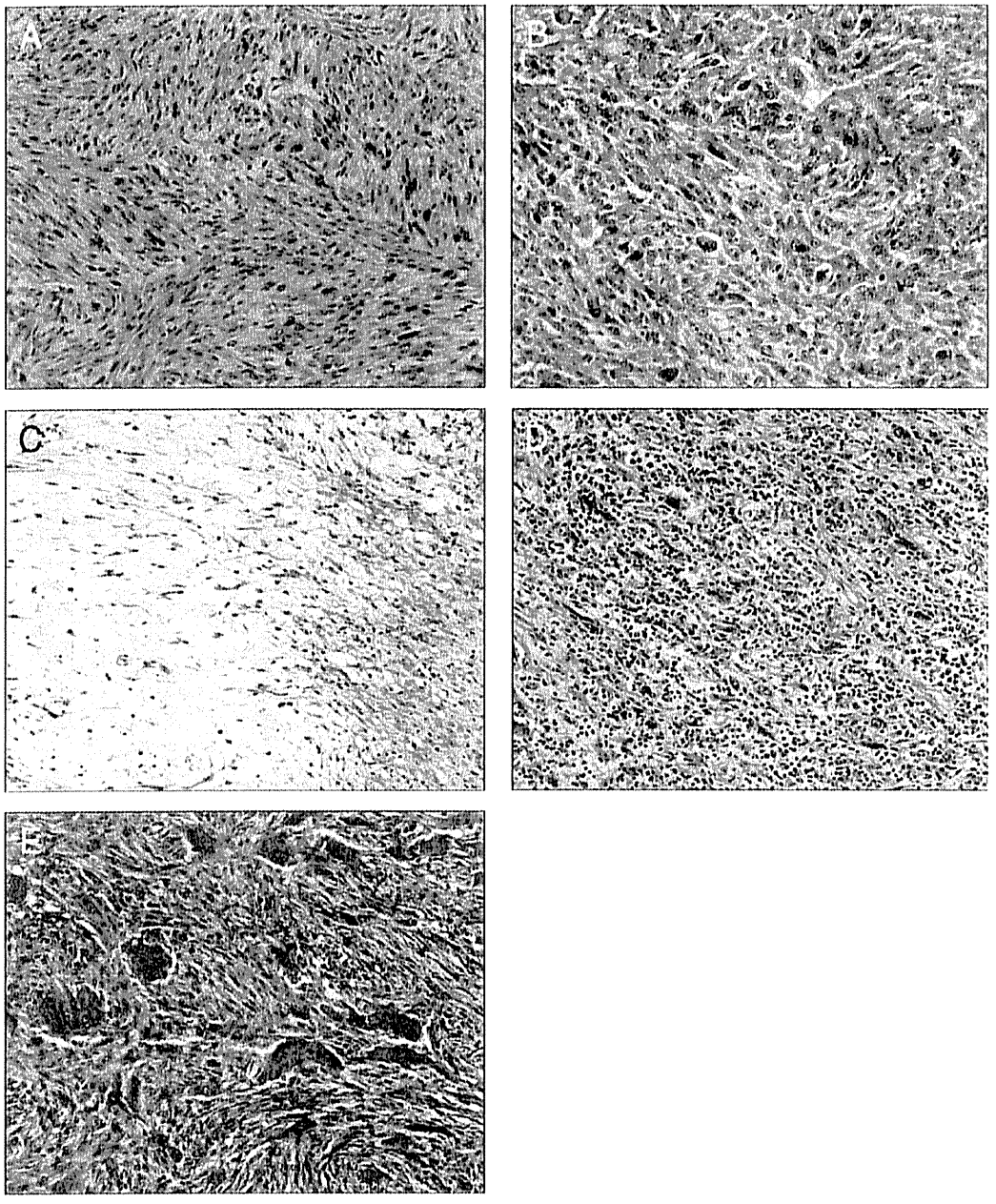

Figure 1. Microscopic features of each type of leiomyosarcoma are shown: (A) classical (conventional) leiomyosarcoma, (B) pleomorphic leiomyosarcoma, (C) leiomyosarcoma with prominent (>50%) myxoid stroma, (D) inflammatory leiomyosarcoma, and (E) leiomyosarcoma with osteoclast-type giant cells.

somatic location, the lower extremity was more likely to be affected than the upper extremity (44 vs 12 cases), and men were more likely to have a tumor in the proximal extremity or trunk (proximal, 44; distal, 6) than women (proximal, 28; distal, 15) ($P = .024$ by chi-square test). Tumors of large-vessel origin in our study included 3 cases of inferior vena cava (male, 1; female, 2) and 1 case of pulmonary artery (female, 1). Positive surgical margin is significantly associated with retroperitoneal and large vessel location ($P = .0001$).

Survival data analysis yielded a disease-specific 5-year survival rate of 50.1%. In univariate analysis, deep

Table 3. Immunohistochemical Results and Statistical Analysis

Analysis	Group	No.	PTEN$^-$, *P*	pAkt$^+$, *P*	pmTOR$^+$, *P*	pS6$^+$, *P*	p4E-BP1$^+$, *P*
Analysis in entire 145 samples including primary, recurrent, and metastatic lesions							
PTEN	–	27	–	–	–	–	–
	+	110					
	N/A	8					
pAkt	+	108 (62)	.7829	–	–	–	–
	–	30					
	N/A	7					
pmTOR	+	98 (47)	>.9999	<.0001[a]	–	–	–
	–	37					
	N/A	10					
pS6	+	105 (86)	>.9999	<.0001[a]	<.0002[a]	–	–
	–	36					
	N/A	4					
p4E-BP1	+	98 (78)	>.9999	<.0001[a]	<.0001[a]	.0490[a]	–
	–	41					
	N/A	6					
Necrosis[b]			.2402	.9836	.1859	.0770	.9853
Mitotic activity[b]			.6359	<.0001[a]	<.0001[a]	.0096[a]	.0005[a]
MIB-1 LI			.3405	<.0001[a]	<.0001[a]	.0032[a]	<.0001[a]
FNCLCC[b]			.6674	.0045[a]	.0011[a]	.0011[a]	.0440[a]
Analysis in 129 samples of primary tumors							
Sex			.1934	.8333	.6856	>.9999	>.9999
Age			.8953	.6733	.5408	.0699	.1196
Location[c]			.7878	.3809	.5851	.2507	.0150[d]
Subtype[c]			.5521	.7295	.1061	.0471[d]	.7606
Depth			.3853	.0321[a]	.2672	.0064[a]	.5087
Diameter			.1874	.3730	.8253	.0398[a]	>.9999
AJCC 6th ed[b]			.6300	.0535	.1951	.0020[a]	.1608
AJCC 7th ed[b]			.9286	.0824	.0231[a]	.0234[a]	.0642
Overall survival			.0472[a]	.0007[a]	.0013[a]	.0015[a]	.0124[a]
Event-free survival			.0060[a]	.0002[a]	.0079[a]	.0022[a]	.0080[a]

Abbreviations: 4E-BP1, eukaryotic translation initiation factor 4E-binding protein; AJCC, American Joint Committee on Cancer; FNCLCC, French Federation of Cancer Centers; LI, labeling index; mTOR, mammalian target of rapamycin; N/A, not available; p, phosphorylated; PTEN, phosphatase and tensin homologue. Fisher exact test or log-rank test was used, if not mentioned. Parenthetical figures represent the number of cases in which >50% of the tumor cells were immunohistochemically positive.

[a] Statistically significant.

[b] Mann-Whitney *U* test.

[c] Chi-square test.

[d] *P* values from the chi-square test are displayed. Tukey multiple comparison test showed no significant difference between any 2 groups.

location, large-vessel origin, positive surgical margin, higher mitotic activity (the number of mitoses per optical field), high MIB-1 LI, existence of tumor necrosis, higher French Federation of Cancer Centers grade, and higher AJCC sixth edition stage were prognostic risk factors. That AJCC seventh edition stage was not a significant prognostic factor might derive from the assignment to stages I and II. AJCC sixth edition stage can reflect depth and size of the tumor, but AJCC seventh edition reflects only histological differentiation between stages I and II, and thus the small number of well-differentiated leiomyosarcomas (AJCC seventh edition stage I) in our series might have influenced the prognostic analyses. With regard to the histological subtypes, pleomorphic LMS, LMS with giant cells, and LMS with myxoid area showed worse prognosis than classical LMS. LMS with giant cells was characterized by a high rate of recurrence or metastasis (6 of 6 cases: 2 recurrences, 2 lung metastases, 1 soft tissue metastasis, 1 metastasis not described in detail).

Immunohistochemistry

The results of immunostaining for PTEN, pAkt, pmTOR, pS6, and p4E-BP1 and the correlation between them and with clinicopathological data are summarized in

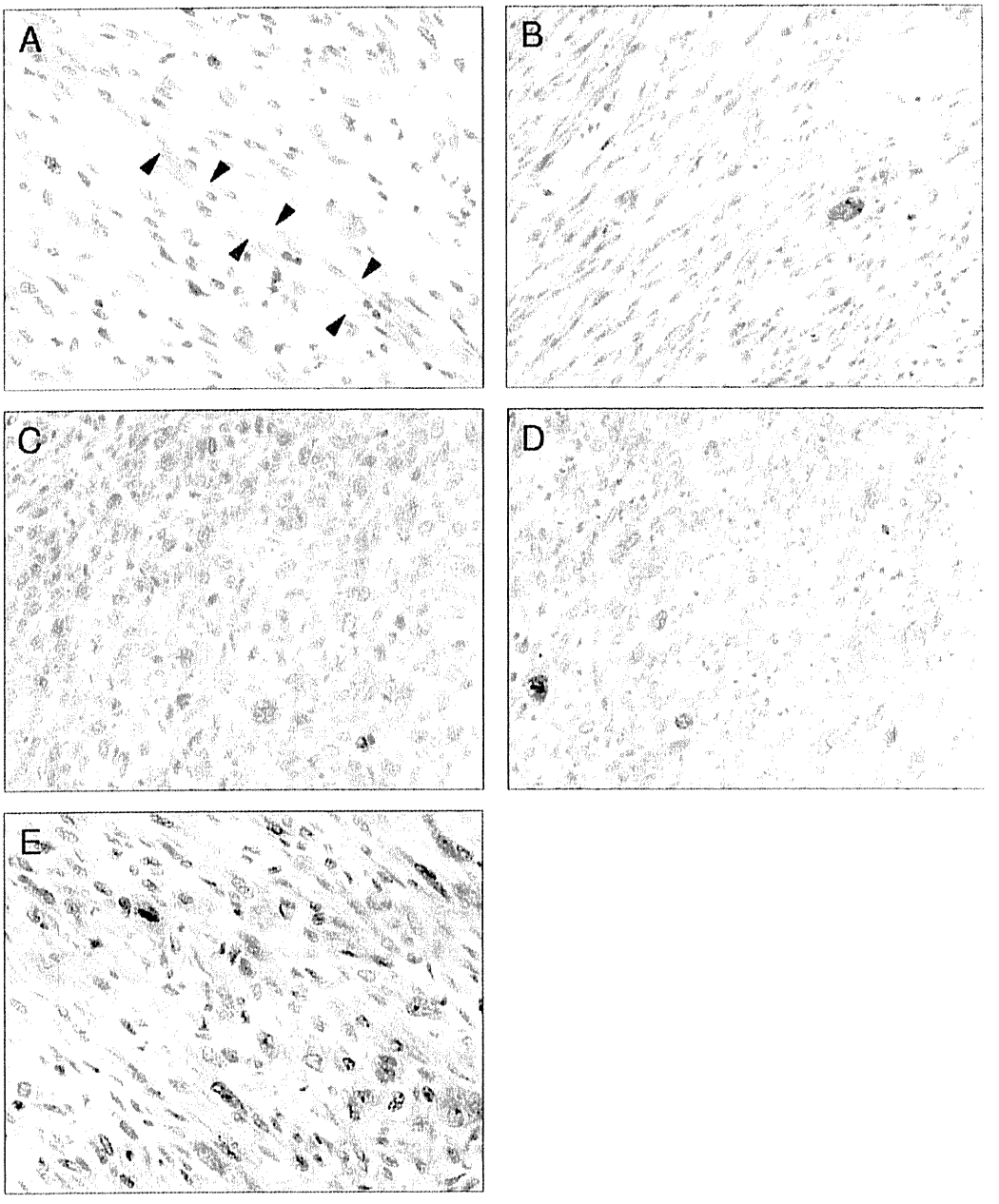

Figure 2. The results of immunohistochemical study are shown: (A) decreased expression of phosphatase and tensin homologue in the tumor cells and immunostaining of endothelial cells (arrowhead); and immunopositivity of phosphorylated (B) Akt, (C) mammalian target of rapamycin, (D) S6, and (E) eukaryotic translation initiation factor 4E-binding protein. Immunostaining for each antibody was recognized mainly in the cytoplasm.

Table 3. Only 19.7% of tumors showed negative PTEN expression (Fig. 2A), whereas the majority of the LMS cases were positive for pAkt, pmTOR, pS6, and p4E-BP1 (Fig. 2B-E) (78.3%, 72.6%, 74.5%, and 70.5%, respectively). Positive staining of all the antibodies used in this study was recognized mainly in the cytoplasm of LMS cells. The cases in which EC failed to reveal any staining were excluded from evaluation (PTEN, 8; pAkt, 7; pmTOR, 10; pS6, 4; p4E-BP1, 6 cases). As for the cases with a pleomorphic area, there was no significant

difference in immunostaining pattern between the pleomorphic area and conventional leiomyosarcomatous area in each of the cases.

As shown in Table 3, the positivities for pAkt, pmTOR, pS6, and p4E-BP1 were correlated with each other, whereas PTEN expression did not show significant correlation with any molecules along the Akt/mTOR pathway. The positivities for pAkt, pmTOR, pS6, and p4E-BP1 were correlated with higher mitotic activity and MIB-1 LI $\geq$30%. Moreover, pAkt$^+$ was significantly correlated with deep tumor location, high French Federation of Cancer Centers grade, and AJCC seventh edition stage, and pS6$^+$ was correlated with deep tumor location, large tumor size, high French Federation of Cancer Centers grade, and high AJCC sixth and seventh edition stage.

The correlations between the immunohistochemical results and disease-specific or event-free survival were evaluated in the 129 primary tumors. Immunopositivity for pAkt, pmTOR, pS6, and p4E-BP1 and negative staining for PTEN were significant risk factors of poorer prognosis (disease-specific survival and event-free survival) (Table 3). The Kaplan-Meier survival curves for disease-specific survival according to the immunohistochemical results are displayed in Figure 3. No prognostic differences were revealed in any of the molecules between score 1 and 2. Correspondent metastatic lesions were also analyzed in 6 cases and local recurrences in 10 cases. There was no significant difference in immunostaining pattern between primary lesions and recurrent or metastatic lesions (data not shown).

Benign smooth muscle tumors showed positive immunostaining for pAkt, pmTOR, pS6, and p4E-BP1 in 25%, 25%, 38%, and 0%, respectively. One case of 8 was negative for PTEN (13%). Compared with benign tumors, LMS showed significantly frequent overexpression of pAkt ($P = .0030$), pmTOR ($P = .0094$), pS6 ($P = .0495$), and p4E-BP1 ($P = .0001$) by Fisher exact test.

Multivariate Analysis

In the clinicopathological parameters, multivariate analysis showed that tumor location, tumor necrosis, and higher mitotic activity were poor prognostic risk factors for disease-specific survival, and tumor location, histological subtypes, and higher mitotic activity were poor prognostic risk factors for event-free survival (Table 4). MIB-1 LI, French Federation of Cancer Centers grade, and AJCC grade were excluded in this multivariate analysis, because they are determined or affected by other parameters. Each immunohistochemical parameter was adjusted by the above 4 clinicopathological factors (tumor necrosis, mitotic activity, tumor location, and histological subtypes) (Table 5), and the multivariate analysis showed that pAkt$^+$, mTOR$^+$, and pS6$^+$ were significantly poor prognostic factors for disease-specific survival, and PTEN$^-$, pAkt$^+$, and p4E-BP1$^+$ were significantly poor prognostic risk factors for event-free survival.

Western Blotting

Pan-Akt and pAkt were detected in all the tumor samples. Densitometric analysis demonstrated that Akt was phosphorylated to a 0.9 to 4.1 (mean, 1.7 $\pm$ 0.82)-fold higher extent in tumor samples than in non-neoplastic tissue (Fig. 4). The extent of phosphorylation of Akt was calculated as follows, compared with normal tissue in each case: (pAkt [tumor] / pan-Akt [tumor]) $\times$ (pan-Akt [normal] / pAkt [normal]). The samples that were immunohistochemically pAkt$^+$ showed higher score (mean, 2.0 $\pm$ 0.88) than immunohistochemically negative samples (mean, 1.1 $\pm$ 0.28) ($P = .0205$ by Mann-Whitney U test). Pan-mTOR was detected in all the tumor samples and pmTOR in 10 of the 13 tumor samples. In contrast, normal samples rarely showed pmTOR expression, and thus phosphorylation of mTOR was evaluated as follows: pmTOR (tumor) / pan-mTOR (tumor), adjusted by the loading control, with a maximal value of 1.0. The samples that were immunohistochemically pmTOR$^+$ showed higher scores (mean, 0.67 $\pm$ 0.32) than the negative samples (mean, 0.39 $\pm$ 0.26), but this was not statistically significant ($P = .1612$). pS6 was detected in 9 of the 13 tumor samples, but not in any normal tissue samples.

Mutational Analysis

We found no mutation (0 of 39 cases) around the hot spots in *AKT1* (E17) or *PIK3CA* (E542, E545, and H1047) by direct DNA sequencing analyses.

DISCUSSION

The Akt/mTOR pathway appears to play a central role in the development of multiple neoplasms.[21-23] The present study aimed to investigate the mechanism of activation of the Akt/mTOR pathway and its engagement in clinical and histopathological behaviors in a large series of soft tissue LMS.

Soft tissue LMS has clinical differences according to its location.[24,25] Deep location was a prognostic risk factor in our univariate analysis. Tumor location in large vessels was another prognostic risk factor in our series, as well as Hines's report in leiomyosarcoma of the inferior vena

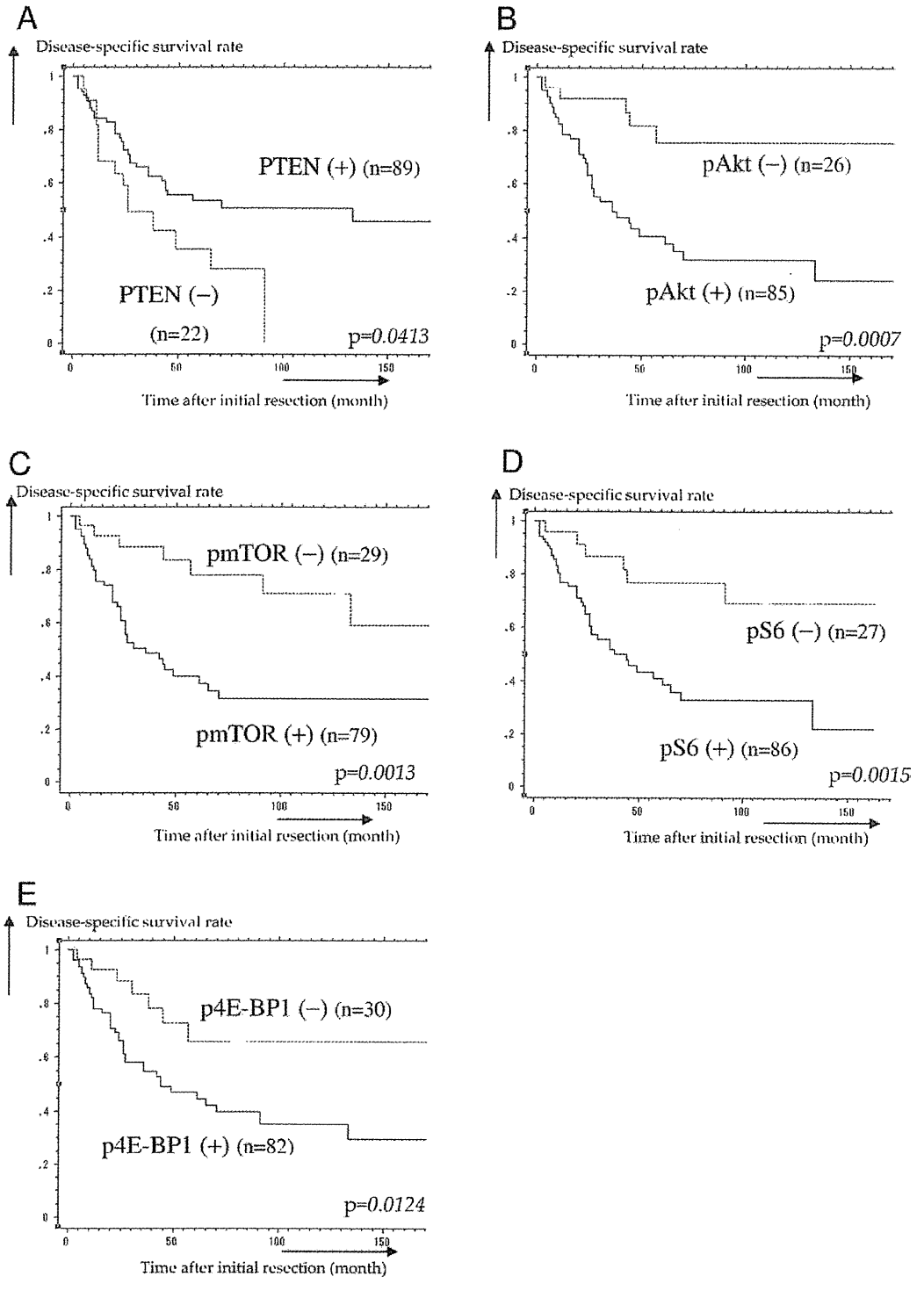

Figure 3. Kaplan-Meier survival curves for disease-specific survival according to the results of immunohistochemical study are shown: (A) phosphatase and tensin homologue (PTEN), (B) phosphorylated Akt, (C) phosphorylated mammalian target of rapamycin (pmTOR), (D) pS6, and (E) phosphorylated eukaryotic translation initiation factor 4E-binding protein (p4E-BP1). All the antibodies were correlated with disease-specific survival by log-rank test ($P < .05$).

cava.[26] As to the poor prognostic factors among the pathological parameters, higher mitotic activity, existence of tumor necrosis, and histological subtypes (pleomorphic LMS, LMS with giant cells, and LMS with myxoid area) were proposed as prognostic risk factors in this study. Pleomorphic LMS and its clinically aggressive character in the present study was consistent with our previous report.[16] LMS with osteoclastlike giant cells has been well documented by Fletcher et al.[27,28] The prognostic significance of this histology, however, has remained unclear. In the present series, we described a high rate of recurrence and metastasis and a worse survival rate compared with classical LMS and revealed that LMS with giant cells has

Table 4. Multivariate Survival Analysis for Clinicopathological Parameters in 129 Primary Tumors

Parameter	Disease-Specific Survival, *P*	Event-Free Survival, *P*
Sex	.7966	.3632
Age	.3339	.3374
Depth	.7428	.9869
Diameter	.6911	.5544
Surgical margin	.6633	.1945
Location	.0062[a,b]	.0046[a,c]
Subtype[d]	.2670	.0013[a,e]
Necrosis	.0004[a]	.0641
Mitotic activity	<.0001[a]	<.0001[a]

The Weibull model was used for multivariate analysis.
[a] Statistically significant.
[b] Large vessel location (V) showed significantly worse prognosis than the other groups: retroperitoneal (R) ($P = .0216$), proximal extremities and trunk (P) ($P = .0048$), and distal extremities (D) ($P = .0006$).
[c] Group V showed significantly worse prognosis than P ($P = .0225$) and D ($P = .0046$).
[d] Histological subtypes were categorized into 4 groups (pleomorphic type, giant cell type, >50% myxoid area, and others).
[e] Giant cell type showed significantly worse prognosis than the other groups: pleomorphic type ($P = .0002$), >50% myxoid area ($P = .0083$), and others ($P = .0002$).

Table 5. Multivariate Survival Analysis for Immunohistochemical Parameters in 129 Primary Tumors Adjusted by Tumor Necrosis, Mitotic Activity, Location, and Histological Subtypes[a]

Parameter	Disease-Specific Survival, *P*	Event-Free Survival, *P*
$PTEN^-$	.2647	.0109[b]
$pAkt^+$	.0040[b]	.0006[b]
$pmTOR^+$	.0447[b]	.1284
$pS6^+$	.0406[b]	.0566
$p4E\text{-}BP1^+$	.0844	.0154[b]

Abbreviations: 4E-BP1, eukaryotic translation initiation factor 4E-binding protein; mTOR, mammalian target of rapamycin; p, phosphorylated; PTEN, phosphatase and tensin homologue.
The Weibull model was used for multivariate analysis.
[a] Histological subtypes were categorized into 4 groups (pleomorphic type, giant cell type, >50% myxoid area, and others).
[b] Statistically significant.

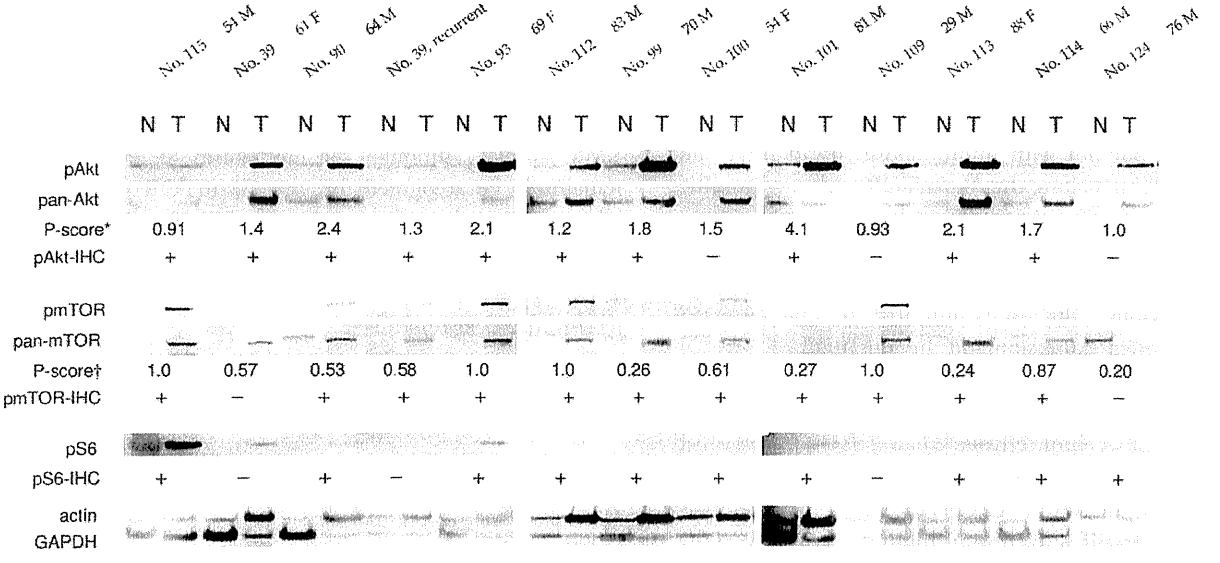

Figure 4. Phosphorylated (p) Akt and pan-Akt were detected in all the tumor samples. Densitometric analysis demonstrated that Akt was phosphorylated to a 0.9 to 4.1 (mean, 1.7)-fold higher extent in tumor samples than in non-neoplastic tissue. Phosphorylated mammalian target of rapamycin (pmTOR) was detected in 10 of the 13 tumor samples. In contrast, normal samples rarely showed pmTOR expression. pS6 was also detected in 9 of the 13 tumor samples, but not in any normal tissue samples. GAPDH, glyceraldehyde-3-phosphate dehydrogenase; IHC, Immunohistochemistry. P-score refers to phosphorylation score, which was calculated as follows: *(pAkt [tumor] / pan-Akt [tumor]) × (pan-Akt [normal]/pAkt [normal]); †pmTOR (tumor) / pan-mTOR (tumor).

aggressive behavior. We also demonstrated that LMS with a prominent (>50%) myxoid area was associated with shorter disease-specific survival. Four of the 5 cases with a prominent myxoid area had died of the disease within 4 years, with the exception being a patient with definitive myxoid LMS, who has so far achieved a 75-month event-free survival. Myxoid LMS of soft tissue, which has less atypia and pleomorphism and tends to locate in the vulva and vagina, should be distinguished from LMS with myxoid area.

Phosphorylation of kinases along the Akt/mTOR pathway reflects their activated status. We demonstrated activation of the Akt/mTOR pathway in LMS by an immunohistochemical study in which pAkt, pmTOR, pS6, and p4E-BP1 were positive in most cases and were correlated with one another's immunopositivity, higher mitotic activity, higher MIB-1 LI, and worse prognosis. Moreover, the levels of positivity for pAkt, pmTOR, pS6, and p4E-BP1 were higher than in benign smooth muscle tumors of soft tissue. Immunoblotting also showed that Akt and mTOR were phosphorylated in the majority of tumor samples and to a higher extent than in non-neoplastic tissue. The results of immunoblotting seemed to correspond with the immunohistochemical findings, but these associations were not statistically significant in pmTOR, probably because of the small number of frozen specimens.

Abnormalities of several molecules could be responsible for activation of the Akt/mTOR pathway. In the present study, we investigated PTEN protein expression immunohistochemically and found that the loss of PTEN expression was not the major event in LMS. We also revealed that the loss of PTEN was correlated with worse prognosis but not with immunopositivity of pAkt and other molecules along the Akt/mTOR pathway. Another factor that might activate this pathway is a mutation in *PIK3CA* or in *AKT1*. We performed direct DNA sequencing analyses for these mutations, but did not find any mutations. Our results indicated that the decreased PTEN protein expression and the mutations of *PIK3CA* or *AKT1* might not make major contributions to activation of the Akt/mTOR pathway. Another potential factor, activation of receptor tyrosine kinases, has been described in the literature. Several receptor tyrosine kinases upstream of the Akt/mTOR pathway have been reported to show aberrant activation in multiple neoplasms. Epidermal growth factor receptor (EGFR) is among these receptors. Dobashi et al investigated mutation and amplification of EGFR in bone and STS.[29] Their sarcoma series included only 1 LMS, which showed no protein overexpression, mutation, or amplification of EGFR. More studies are needed to investigate the contribution of EGFR activation to the development and progression in LMS. Another potential tyrosine kinase receptor is insulinlike growth factor 1 (IGF1) receptor. Studies of uterine LMS have indicated that IGF2 is highly expressed and might result in activation of PI3K through the IGF1 receptor.[30] The mutation of k-*ras*, also upstream of PI3K, could activate the Akt/mTOR pathway.[31] K-*ras* mutation has been reported in a certain proportion (7%-33%) of soft tissue LMS[32,33] and might be a factor in Akt/mTOR pathway activation.

The present study concentrated on analysis in clinical samples, and we could not find an available LMS cell line of soft tissue origin. The establishment of cell lines from soft tissue LMS would allow further investigation into the role and mechanisms of Akt/mTOR pathway activation. Despite this limitation, the present study may have important clinical and therapeutic implications, because of the potential of the Akt/mTOR pathway as a therapeutic target. In fact, mTOR inhibitors such as RAD001 (everolimus) have been proven to be effective against several human neoplasms.[34,35] Moreover, recent studies using a dual inhibitor of mTOR and PI3K have provided supportive evidence for this strategy.[36,37] Thus, our study encourages the application of such inhibitors to the treatment of soft tissue LMS.

In conclusion, we revealed that the Akt/mTOR pathway was activated and was correlated with worse clinical prognosis and pathological behavior. The decrease of PTEN protein expression did not seem to be responsible for this activation, and mutations around the hot spots of *AKT1* and *PIK3CA* were not identified in our soft tissue LMS samples. Although the mechanism of activation remains to be accounted for, the Akt/mTOR pathway plays a major role in the progression of LMS and has the potential to be a therapeutic target.

FUNDING SOURCES

Y.O. is supported by a Grant-in-Aid for Scientific Research (B) (No. 21390107) from the Japan Society for the Promotion of Science.

CONFLICT OF INTEREST DISCLOSURES

The authors made no disclosures.

REFERENCES

1. Oda Y, Tamiya S, Oshiro Y, et al. Reassessment and clinicopathological prognostic factors of malignant fibrous histiocytoma of soft parts. *Pathol Int.* 2002;52:595-606.

2. Hennessy BT, Smith DL, Ram PT, Lu Y, Mills GB. Exploiting the PI3K/AKT pathway for cancer drug discovery. *Nat Rev Drug Discov.* 2005;4:988-1004.
3. Altomare DA, Testa JR. Perturbations of the AKT signaling pathway in human cancer. *Oncogene.* 2005;24:7455-7464.
4. Khaleghpour K, Pyronnet S, Gingras AC, Sonenberg N. Translational homeostasis: eukaryotic translation initiation factor 4E control of 4E-binding protein 1 and p70 S6 kinase activities. *Mol Cell Biol.* 1999;19:4302-4310.
5. Gingras AC, Raught B, Sonenberg N. Regulation of translation initiation by FRAP/mTOR. *Genes Dev.* 2001;15:807-826.
6. Ruvinsky I, Meyuhas O. Ribosomal protein S6 phosphorylation: from protein synthesis to cell size. *Trends Biochem Sci.* 2006;31:342-348.
7. Tomita Y, Morooka T, Hoshida Y, et al. Prognostic significance of activated AKT expression in soft-tissue sarcoma. *Clin Cancer Res.* 2006;12:3070-3077.
8. Dobashi Y, Suzuki S, Sato E, Hamada Y, Yanagawa T, Ooi A. EGFR-dependent and independent activation of Akt/mTOR cascade in bone and soft tissue tumors. *Mod Pathol.* 2009;22:1328-1340.
9. Maehama T, Dixon JE. The tumor suppressor, PTEN/MMAC1, dephosphorylates the lipid second messenger, phosphatidylinositol 3,4,5-trisphosphate. *J Biol Chem.* 1998;273:13375-13378.
10. Kawaguchi K, Oda Y, Saito T, et al. Genetic and epigenetic alterations of the PTEN gene in soft tissue sarcomas. *Hum Pathol.* 2005;36:357-363.
11. Samuels Y, Wang Z, Bardelli A, et al. High frequency of mutations of the PIK3CA gene in human cancers. *Science.* 2004;304:554.
12. Samuels Y, Diaz LA Jr, Schmidt-Kittler O, et al. Mutant PIK3CA promotes cell growth and invasion of human cancer cells. *Cancer Cell.* 2005;7:561-573.
13. Kang S, Bader AG, Vogt PK. Phosphatidylinositol 3-kinase mutations identified in human cancer are oncogenic. *Proc Natl Acad Sci U S A.* 2005;102:802-807.
14. Carpten JD, Faber AL, Horn C, et al. A transforming mutation in the pleckstrin homology domain of AKT1 in cancer. *Nature.* 2007;448:439-444.
15. Evans HL, Shipley J. Leiomyosarcoma. In: Fletcher CD, Unni KK, Mertens FE, eds. World Health Organization Classification of Tumours. Pathology and Genetics of Tumours of Soft Tissue and Bone. Lyon, France: IARC Press; 2002:131-134.
16. Oda Y, Miyajima K, Kawaguchi K, et al. Pleomorphic leiomyosarcoma: clinicopathologic and immunohistochemical study with special emphasis on its distinction from ordinary leiomyosarcoma and malignant fibrous histiocytoma. *Am J Surg Pathol.* 2001;25:1030-1038.
17. Edge SB, Byrd DR, Compton CC, Fritz AG, Greene FL, Trotti A. AJCC Cancer Staging Manual. 7th ed. St Louis, MO: Springer; 2010.
18. Greene FL, Page DL, Fleming ID, Fritz AG, Balch CM. AJCC Cancer Staging Manual. 6th ed. St Louis, MO: Springer; 2002.
19. Dormond O, Madsen JC, Briscoe DM. The effects of mTOR-akt interactions on anti-apoptotic signaling in vascular endothelial cells. *J Biol Chem.* 2007;282:23679-23686.
20. Dunlap J, Le C, Shukla A, et al. Phosphatidylinositol-3-kinase and AKT1 mutations occur early in breast carcinoma. *Breast Cancer Res Treat.* 2010;120:409-418.
21. Balsara BR, Pei J, Mitsuuchi Y, et al. Frequent activation of AKT in non-small cell lung carcinomas and preneoplastic bronchial lesions. *Carcinogenesis.* 2004;25:2053-2059.
22. Nathan CO, Amirghahari N, Abreo F, et al. Overexpressed eIF4E is functionally active in surgical margins of head and neck cancer patients via activation of the Akt/mammalian target of rapamycin pathway. *Clin Cancer Res.* 2004;10:5820-5827.
23. Lin HJ, Hsieh FC, Song H, Lin J. Elevated phosphorylation and activation of PDK-1/AKT pathway in human breast cancer. *Br J Cancer.* 2005;93:1372-1381.
24. Weiss SW, Goldblum JR. Leiomyosarcoma. In: Weiss SW, Goldblum JR, eds. Enzinger and Weiss's Soft Tissue Tumors. 5th ed. Philadelphia, PA: Mosby; 2007:545-564.
25. Svarvar C, Bohling T, Berlin O, et al. Clinical course of nonvisceral soft tissue leiomyosarcoma in 225 patients from the Scandinavian sarcoma group. *Cancer.* 2007;109:282-291.
26. Hines OJ, Nelson S, Quinones-Baldrich WJ, Eilber FR. Leiomyosarcoma of the inferior vena cava: prognosis and comparison with leiomyosarcoma of other anatomic sites. *Cancer.* 1999;85:1077-1083.
27. Fletcher CD. Leiomyosarcoma with osteoclast-like giant cells. *Histopathology.* 1993;22:94-95.
28. Mentzel T, Calonje E, Fletcher CD. Leiomyosarcoma with prominent osteoclast-like giant cells. Analysis of 8 cases closely mimicking the so-called giant cell variant of malignant fibrous histiocytoma. *Am J Surg Pathol.* 1994;18:258-265.
29. Dobashi Y, Suzuki S, Sugawara H, Ooi A. Involvement of epidermal growth factor receptor and downstream molecules in bone and soft tissue tumors. *Hum Pathol.* 2007;38:914-925.
30. Rikhof B, de Jong S, Suurmeijer AJ, Meijer C, van der Graaf WT. The insulin-like growth factor system and sarcomas. *J Pathol.* 2009;217:469-482.
31. Uchida A, Hirano S, Kitao H, et al. Activation of downstream epidermal growth factor receptor (EGFR) signaling provides gefitinib-resistance in cells carrying EGFR mutation. *Cancer Sci.* 2007;98:357-363.
32. Hill MA, Gong C, Casey TJ, et al. Detection of K-ras mutations in resected primary leiomyosarcoma. *Cancer Epidemiol Biomarkers Prev.* 1997;6:1095-1100.
33. Yoo J, Robinson RA. H-ras and K-ras mutations in soft tissue sarcoma: comparative studies of sarcomas from Korean and American patients. *Cancer.* 1999;86:58-63.
34. Motzer RJ, Escudier B, Oudard S, et al. Efficacy of everolimus in advanced renal cell carcinoma: a double-blind, randomised, placebo-controlled phase III trial. *Lancet.* 2008;372:449-456.
35. Soria JC, Shepherd FA, Douillard JY, et al. Efficacy of everolimus (RAD001) in patients with advanced NSCLC previously treated with chemotherapy alone or with chemotherapy and EGFR inhibitors. *Ann Oncol.* 2009;20:1674-1681.
36. Maira SM, Stauffer F, Brueggen J, et al. Identification and characterization of NVP-BEZ235, a new orally available dual phosphatidylinositol 3-kinase/mammalian target of rapamycin inhibitor with potent in vivo antitumor activity. *Mol Cancer Ther.* 2008;7:1851-1863.
37. Cao P, Maira SM, Garcia-Echeverria C, Hedley DW. Activity of a novel, dual PI3-kinase/mTor inhibitor NVP-BEZ235 against primary human pancreatic cancers grown as orthotopic xenografts. *Br J Cancer.* 2009;100:1267-1276.

Skeletal Radiol
DOI 10.1007/s00256-011-1337-6

CASE REPORT

Leiomyosarcoma in the humerus with leukocytosis and elevation of serum G-CSF

Takeaki Ishii · Akio Sakamoto · Shuichi Matsuda · Yoshihiro Matsumoto · Katsumi Harimaya · Yusuke Takahashi · Yoshinao Oda · Yukihide Iwamoto

Received: 6 July 2011 / Revised: 2 November 2011 / Accepted: 21 November 2011

Abstract Leukocytosis associated with secretion of granulocyte colony-stimulating factor (G-CSF) has been reported in various tumors, primarily poorly differentiated epithelial tumors, but is extremely rare in bone tumors. An 84-year-old woman experienced swelling and pain in the shoulder for 1 month. Leukocytosis and elevated serum G-CSF were observed, but resolved following tumor resection. A diagnosis of leiomyosarcoma of the bone with expression of G-CSF was confirmed immunohistochemically. Histological diagnosis of leiomyosarcoma showed it to be differentiated, which is unusual for G-CSF–secreting tumors.

Keywords Leiomyosarcoma · Bone · Granulocyte colony-stimulating factor · Leukocytosis

Introduction

Tumors that secrete granulocyte colony-stimulating factor (G-CSF) are characterized by leukocytosis and consist of various types, but in most cases they are epithelial malignancies [1–6] and are characterized by poor differentiation [7]. Among nonepithelial malignancies, or sarcoma, G-CSF–secreting tumors are rare, especially in the bone. Only a few cases of G-CSF–secreting bone tumors have been reported in the English literature. These tumors were characterized by poor differentiation, as either dedifferentiated chondrosarcoma [8] or undifferentiated sarcoma [9]. In the current report, we present a case of leiomyosarcoma in the humerus with leukocytosis and elevation of serum G-CSF.

T. Ishii · A. Sakamoto (✉) · S. Matsuda · Y. Matsumoto · K. Harimaya · Y. Iwamoto
Department of Orthopaedic Surgery, Graduate School of Medical Sciences, Kyushu University,
Fukuoka 812-8582, Japan
e-mail: akio@med.kyushu-u.ac.jp

Y. Takahashi · Y. Oda
Department of Anatomic Pathology, Graduate School of Medical Sciences, Kyushu University,
Fukuoka 812-8582, Japan

Case report

An 84-year-old woman was referred to our institute with pain and swelling in the right shoulder. She had a history of a fracture in the proximal humerus and had undergone fixation with a titanium nail at a nearby hospital 4 years earlier (Fig. 1a). No tumors had been previously detected or treated, including uterine leiomyoma. On radiographs, complete bone union was confirmed 1 year after surgery (Fig. 1b). At the first visit to our institute, 3 years later, radiographs showed an osteolytic lesion with an ill-defined margin around the location of the previous fracture site at the proximal humerus (Fig. 1c). Magnetic resonance imaging (MRI) showed a multinodular lesion with low-signal intensity on T1-weighted images and high-signal intensity with a surrounding low-signal intensity capsule-like area on T2-weighted images (Fig. 2a and b). Gadolinium enhancement was observed outside of the central part of each nodule on T1-weighted images (Fig. 2c). The tumor extended to the surrounding muscle, as well as the shoulder joint. Based on these image analyses, possible diagnoses included primary high-grade malignant bone tumor, such as malignant fibrous histiocytoma of bone (undifferentiated pleomorphic sarcoma) or osteosarcoma with reduced osteoid formation, metastatic bone tumor, and infection. [18 F]-2-fluoro-2-deoxy-D-glucose-positron emission tomography (FDG-PET) showed positivity in the proximal humerus; no other lesions were detected.

Published online: 14 December 2011

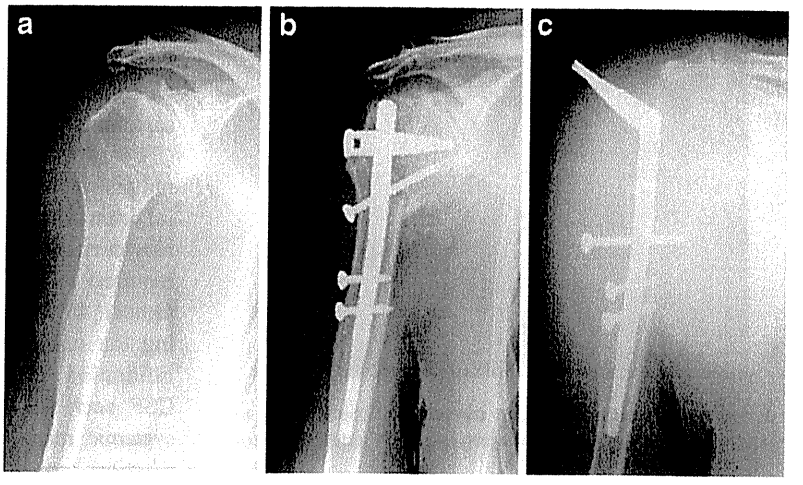

Fig. 1 Radiographs show a right humerus fracture without neoplastic changes (**a**). The fracture was treated with a metallic nail and screws (**b**). Osteolytic changes were observed around the previously fractured lesion at initial presentation (**c**)

Body temperature was normal, and the local heat over the tumor was mild. Laboratory data showed leukocytosis with an increased white blood cell count (17,500/μl) at the initial visit (neutrophils, 77%). The C-reactive protein level was slightly increased (0.47 mg/dl). The bacterial culture of the sample from the lesion was negative. Based on these findings, the possibility of general infection, as well as local infection, was rejected. Histological analysis of a needle biopsy sample suggested a diagnosis of spindle sarcoma. During the 1-month period from the initial visit until tumor resection, the area of osteolysis had expanded, and local symptoms such as swelling, local heat, and pain had advanced rapidly.

Resection including surrounding normal tissue was indicated; this consisted of the affected humerus and the shoulder joint along with surrounding muscle tissue. A diagnosis of leiomyosarcoma of the bone was made. The tumor was composed of spindle cells in fascicles, and the tumor cells had characteristic blunt-ended nuclei (Fig. 3). Immunohistochemically, the tumor cells were positive for muscle-specific actin (HHF35) and calponin, a cytoskeleton-associated actin-binding protein that is a more specific myogenic marker (Fig. 4a and b).

At the time of surgery, the white blood cell count was 22,900/μl (neutrophils, 86%), and the G-CSF serum level was elevated (153 pg/ml; normal, <39 pg/ml). G-CSF expression was confirmed in the resected tissue section immunohistochemically (Fig. 4c). One month after surgery, the white blood cell count and G-CSF serum level had returned to normal values (white blood cells, 4,900/μl; neutrophils, 63%; G-CSF, 19.5 pg/ml) (Fig. 5). There was no sign of recurrence at 12-month follow-up. The patient was informed that data from her case would be submitted for publication, and she provided her consent.

Discussion

G-CSF–secreting tumors are characterized by leukocytosis. In the current case, leukocytosis and a high G-CSF serum

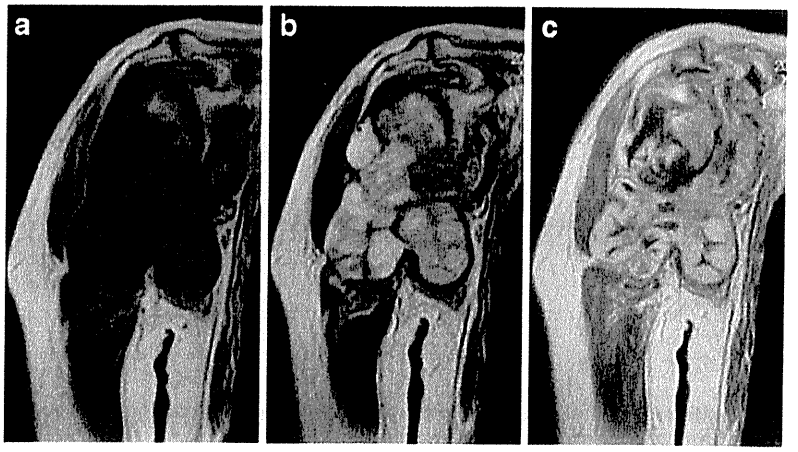

Fig. 2 MRI shows a lobulated lesion with low T1-weighted (**a**), high T2-weighted (**b**), and gadolinium-enhanced T1-weighted (**c**) images at initial presentation

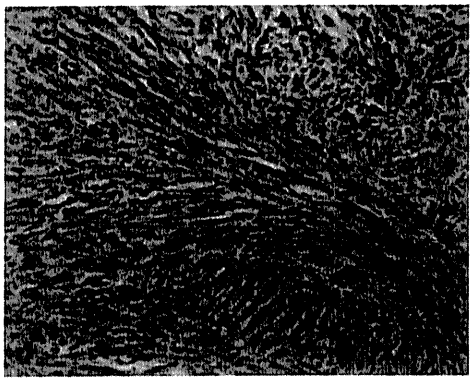

Fig. 3 Leiomyosarcoma of the bone composed of spindle cells with blunt-ended nuclei arranged in interlacing fascicles (hematoxylin-eosin stain; original magnification, ×250)

level disappeared after tumor resection. G-CSF expression was also confirmed immunohistochemically in the resected tissue section. Accordingly, the current tumor was considered to be a G-CSF–secreting tumor. Various tumors have been reported to express G-CSF; however, most of these cases have been epithelial malignancies, including gastric carcinoma, hepatocellular carcinoma, bladder cancer, uterine cervical cancer, and thymic squamous cell carcinoma [1–6], and are characterized by poor differentiation [7]. The current case was diagnosed as leiomyosarcoma of bone. Leiomyosarcoma of bone is considered to be a very rare malignant tumor [10]; thus, we excluded metastatic leiomyosarcoma, especially from possible uterine leiomyosarcoma. FDG-PET has been reported to be useful for diagnosing uterine tumor. Uterine malignancy is characterized by high FDG uptake, and even benign uterine leiomyomas usually show mild FDG uptake [11]. In the current case, the patient did not have a past history of uterine tumor, and FDG-PET only showed accumulation in the humerus tumor. Therefore, we concluded that the humerus lesion was a primary leiomyosarcoma of bone.

Possible local findings in cases of G-CSF–secreting tumors include neutrophilic infiltration and subsequent inflammatory reaction, due to the properties of G-CSF. However, no specific clinical image features have been reported to our knowledge in cases of G-CSF–secreting tumors. In the current case, the area of edema surrounding the tumor was not wide on MRI, and neutrophilic infiltration was inconspicuous in the resected section. G-CSF secretion by tumors results in leukocytosis as a systemic reaction, but may not cause any specific local reaction, considering the pathological findings in the current case.

In most previous reports, G-CSF expression in tumor cells was associated with aggressive features and poor prognosis. Some reports have indicated that G-CSF can support the growth of osteosarcoma and Ewing sarcoma [12, 13]. In contrast, G-CSF expression was not found to be an adverse prognostic factor in ovarian carcinomas [14]. In the current case, although the actual biological behavior is unknown, the increase in tumor size over a short duration suggests that the tumor acquired aggressiveness, possible related to leukocytosis.

In G-CSF–secreting tumors, G-CSF expression has been assumed to occur in advanced stages, characterized by poor differentiation, rather than in early stages, when the tumor is well-differentiated [7]. Leukocytosis has been reported to be an initial sign of aggressive tumor extension. Furthermore, the histological changes that accompany poor differentiation associated with leukocytosis might influence the subsequent virulent clinical

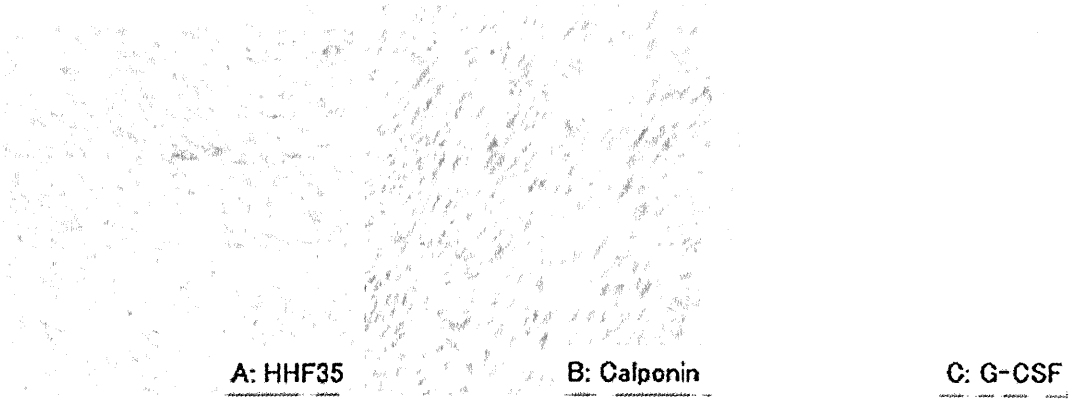

Fig. 4 Leiomyosarcoma of the bone shows positive cytoplasmic immunoreactivity for the myogenic markers HHF35 (**a**) and calponin (**b**), and for G-CSF (**c**) (immunohistochemistry; original magnification, ×300)

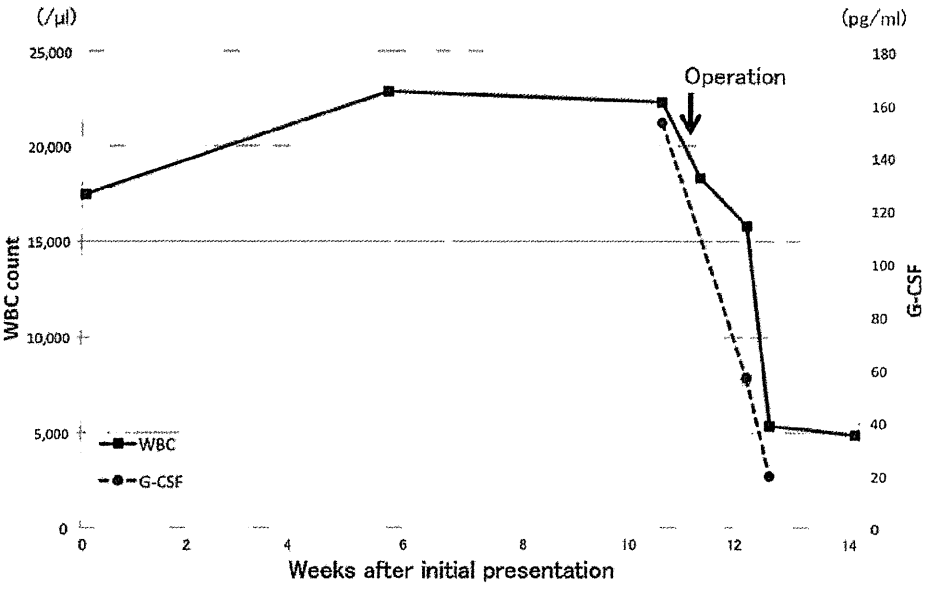

Fig. 5 Time course of white blood cell count and G-CSF serum level. The white blood cell count, including neutrophils, and G-CSF serum levels decreased after surgery

features [15]. Among bone and soft-tissue tumors, G-CSF–secreting tumors have been reported to be associated with undifferentiated tumors [8, 16]. In a previously reported bone tumor case, G-CSF expression was only detected in the dedifferentiated components and not in the well-differentiated components of dedifferentiated chondrosarcoma [8]. In the current case, leiomyosarcoma with preserved differentiation expressed G-CSF during the course of tumor extension. Therefore, it could be assumed that the tumor cells acquired the functionality of G-CSF, possibly related to aggressiveness, without morphological deterioration.

To the best of our knowledge, only two cases of G-CSF–secreting bone tumor have been reported in the English literature [8, 9]. The degree of leukocytosis in the current case was rather mild (about $20\times10^3/\mu l$) in comparison to other reported leukocytosis cases ($>100\times10^3/\mu l$) [7, 16]. Therefore, the possibility of a large number of unreported G-CSF–secreting tumors, including bone tumors, exists. Careful case analysis, especially of malignant tumors with aggressive onset associated with leukocytosis, is required to examine G-CSF expression and to analyze the association between G-CSF function and its malignant behavior.

In summary, we have presented a case report of leiomyosarcoma of the bone with leukocytosis associated with G-CSF expression. The diagnosis of leiomyosarcoma indicates that this tumor was differentiated, which is unusual for a G-CSF–secreting tumor.

Acknowledgments We thank Miss K. Miller (Royal English Language Centre, Fukuoka, Japan) for revising the English used in this manuscript.

References

1. Ayabe E, Kaira K, Takahashi T, Murakami H, Tsuya A, Nakamura Y, et al. Thymic squamous cell carcinoma producing granulocyte colony-stimulating factor associated with a high serum level of interleukin 6. Int J Clin Oncol. 2009;14(6):534–6.
2. Joshita S, Nakazawa K, Koike S, Kamijo A, Matsubayashi K, Miyabayashi H, et al. A case of granulocyte-colony stimulating factor-producing hepatocellular carcinoma confirmed by immunohistochemistry. J Korean Med Sci. 2010;25(3):476–80.
3. Kawaguchi M, Asada Y, Terada T, Takehara A, Munemoto Y, Fujisawa K, et al. Aggressive recurrence of gastric cancer as a granulocyte-colony-stimulating factor-producing tumor. Int J Clin Oncol. 2010;15(2):191–5.
4. Mabuchi S, Matsumoto Y, Morii E, Morishige K, Kimura T. The first 2 cases of granulocyte colony-stimulating factor producing adenocarcinoma of the uterine cervix. Int J Gynecol Pathol. 2010;29(5):483–7.
5. Sawazaki H, Taki Y, Takeuchi H. Granulocyte colony-stimulating factor (G-CSF) producing bladder cancer subsequently developed from recurrent non-muscle invasive bladder cancer. Int J Urol. 2010;17(8):741–2.
6. Takagi Y, Nakamura H, Miwa K, Adachi Y, Fujioka S, Haruki T, et al. A case of G-CSF-producing invasive apical cancer resected following preoperative adjuvant therapy. Thorac Cardiovasc Surg. 2010;58(5):304–6.
7. Yamano T, Morii E, Ikeda J, Aozasa K. Granulocyte colony-stimulating factor production and rapid progression of gastric

cancer after histological change in the tumor. Jpn J Clin Oncol. 2007;37(10):793–6.
8. Sakamoto A, Yamamoto H, Tanaka K, Matsuda S, Harimaya K, Oda Y, et al. Dedifferentiated chondrosarcoma with leukocytosis and elevation of serum G-CSF. A case report. World J Surg Oncol. 2006;4:37.
9. Marui T, Yamamoto T, Akisue T, Hitora T, Yoshiya S, Kurosaka M. Granulocyte colony-stimulating factor-producing undifferentiated sarcoma occurring in previously fractured femur. Arch Pathol Lab Med. 2003;127(4):e186–9.
10. Wirbel RJ, Verelst S, Hanselmann R, Remberger K, Kubale R, Mutschler WE. Primary leiomyosarcoma of bone: clinicopathologic, immunohistochemical, and molecular biologic aspects. Ann Surg Oncol. 1998;5(7):635–41.
11. Kitajima K, Murakami K, Kaji Y, Sugimura K. Spectrum of FDG PET/CT findings of uterine tumors. AJR Am J Roentgenol. 2010;195(3):737–43.
12. Morales-Arias J, Meyers PA, Bolontrade MF, Rodriguez N, Zhou Z, Reddy K, et al. Expression of granulocyte-colony-stimulating factor and its receptor in human Ewing sarcoma cells and patient tumor specimens: potential consequences of granulocyte-colony-stimulating factor administration. Cancer. 2007;110(7):1568–77.
13. Thacker JD, Dedhar S, Hogge DE. The effect of GM-CSF and G-CSF on the growth of human osteosarcoma cells in vitro and in vivo. Int J Cancer. 1994;56(2):236–43.
14. Munstedt K, Hackethal A, Eskef K, Hrgovic I, Franke FE. Prognostic relevance of granulocyte colony-stimulating factor in ovarian carcinomas. Arch Gynecol Obstet. 2010;282(3):301–5.
15. Yabuta M, Takeuchi K, Kitazawa S, Morita H. Leukocytosis as an initial sign of aggressive growth of granulocyte colony-stimulating factor-producing cervical cancer. Int J Gynaecol Obstet. 2010;111(2):181–2.
16. Sakamoto A, Matono H, Yoshida T, Tanaka K, Matsuda S, Oda Y, et al. Dedifferentiated liposarcoma with leukocytosis. A case report of G-CSF-producing soft-tissue tumors, possible association with undifferentiated liposarcoma lineage. World J Surg Oncol. 2007;5:131.

J Orthop Sci
DOI 10.1007/s00776-011-0150-3

CASE REPORT

Hematoma of the ligamentum flavum in the thoracic spine: report of two cases and possible role of the transforming growth factor beta-vascular endothelial growth factor signaling axis in its pathogenesis

Yoshihiro Matsumoto · Toshifumi Fujiwara · Ryuta Imamura · Yuko Okada · Katsumi Harimaya · Toshio Doi · Kenichi Kawaguchi · Seiji Okada · Yuichi Yamada · Yoshinao Oda · Yukihide Iwamoto

Received: 17 May 2011 / Accepted: 11 August 2011

Introduction

Intraspinal hematoma is an uncommon cause of neural compression [1]. Among these hematomas, those in the thoracic ligamentum flavum (LF) are by far the rarest and can generate thoracic myelopathy [2]. This report describes two cases of exceptionally rare ligamentum flavum hematoma (LFH) in the thoracic lesion of patients with subacute onset myelopathy and shows the possible role of the transforming growth factor-beta (TGF-beta)-vascular endothelial growth factor (VEGF) signaling axis in its pathogenesis.

Case reports

Patient 1

A 57-year-old male was referred to the hospital with a gait disturbance and numbness of the lower legs. His symptoms had occurred subacutely with a 4-week history, and he had had no remarkable episodes of trauma. He had hepatitis type C, which had caused cirrhosis of the liver and hepatocelluar carcinoma (HCC). The HCC was treated using transarterial embolization, and no local recurrence or distant metastasis has been observed. There was no history of any previous surgery concerning the spinal lesion. Although he did not have back and leg pain, he exhibited spastic gait and disability of heel and toe standing during the first visit. Sensory loss was not remarkable; however, he experienced dysesthesia in both legs. The patellar tendon and Achilles tendon reflexes were increased bilaterally. No Babinski reflex was observed. Vibration sensation was intact, and no apparent motor weakness in the lower extremities was observed. Bowel and bladder function was also normal. Coagulation studies indicated a decrease in the number of platelets (58,000/mm^3; reference range 140,000–440,000/mm^3), and a slight increase in the prothorombin time (41.6 s; reference range 26.0–41.0 s) and partial thromboplastin time (14.8 s; reference range 10.0–13.5 s).

A plain radiograph of the thoracic spine revealed mild degenerative spondylosis in the thoracolumbar region. Magnetic resonance imaging (MRI) showed spinal cord compression at the T11/12 level caused by a posterior round mass (Fig. 1a–d). This intraspinal and extradural mass appeared to be continuous with the left LF. The mass was centrally hyperintense and marginally hypointense on both the T1- and T2-weighted images, suggesting the existence of an accumulation of extracellular methemoglobin in the mass. The enhancement of the mass was not remarkable after intravenous administration of contrast medium. Postmyelography computerized tomography (CT) indicated a large extradural lesion along with degeneration of the facet joint at the T11/12 level. There was no calcification within the mass (Fig. 2 a, b). These imaging results indicated the mass was an LFH, but distinguishing a hematoma from other etiologies, such as a synovial cyst or metastatic tumor, was difficult.

Y. Matsumoto (✉) · T. Fujiwara · R. Imamura · Y. Okada · K. Harimaya · T. Doi · K. Kawaguchi · S. Okada · Y. Iwamoto
Department of Orthopaedic Surgery,
Graduate School of Medical Sciences, Kyushu University,
3-1-1 Maidashi, Higashi-ku, Fukuoka 812-8582, Japan
e-mail: ymatsu@ortho.med.kyushu-u.ac.jp

Y. Okada · S. Okada · Y. Yamada · Y. Oda
Department of Anatomic Pathology,
Graduate School of Medical Sciences, Kyushu University,
3-1-1 Maidashi, Higashi-ku, Fukuoka 812-8582, Japan

Published online: 31 August 2011